Fabrication and Analysis of Drug-Nanoparticles-Based 3D Scaffolds for Targeted Cancer Treatment

ASHESI UNIVERSITY

CAPSTONE PROJECT

B.Sc. Mechanical Engineering

Emmanuel Fidelis Kashumba

(ID: 07632020)

MAY 2020

ASHESI UNIVERSITY

FABRICATION AND ANALYSIS OF DRUG-NANOPARTICLES-BASED 3D SCAFFOLDS FOR TARGETED CANCER TREATMENT

CAPSTONE PROJECT

Capstone Project submitted to the Department of Engineering, Ashesi University in partial fulfilment of the requirements for the award of Bachelor of Science Degree in Mechanical Engineering.

EMMANUEL FIDELIS KASHUMBA

(ID: 07632020)

MAY 2020

DECLARATION

I hereby declare that this capstone is the result of my own original work and that no part of it has been presented for another degree in this university or elsewhere.

Candidate's Signature: ……

Candidate's Name: ……

Date: ……

I hereby declare that preparation and presentation of this capstone were supervised in accordance with the guidelines on supervision of capstone laid down by Ashesi University College.

Supervisor's Signature: ……

Supervisor's Name: ……

Date: ……

Acknowledgments

The completion of this project was propelled by the unwavering assistive contribution of several individuals worthy of acknowledging. Before acknowledging the individuals, I am humbly thankful to God whose mercy covered every error and whose favour coloured every effort needed to successfully start and complete this project.

I would also like to acknowledge my parents Mr. and Mrs. Fidelis Kashumba for their consistent support to this moment.

My heartfelt gratitude also falls on Dr. Danyuo Yiporo for his constructive feedbacks and overall guidance. His dedication to academia proves to be of a novel stature.

I would also share a word of gratitude with the entire Engineering Department for the necessary practical and theoretical knowledge as well as any other form of assistance, used to formulate and accomplish this project.

Abstract

The mutable nature of cancer has made it one of the toughest diseases to successfully fight against. Due to the aggressive nature of cancer, toxic drugs are administered to stop or slow down the growth of cancerous cells. However, most of the conventional treatment methods lack site targeting and specificity, therefore, affecting any rapidly dividing cells. Destruction of normal cells therefore leads to malfunctioning of body organs. A proposed solution is to use localized drug delivery, with nanocomposite-based scaffolds with tuneable biodegradation, biocompatibility, and porous structures. These drug- and nanoparticle-based scaffolds were fabricated through solvent casting method. Scaffolds containing magnetite nanoparticles were loaded with an experimental drug (Dichapetalin M), Tamoxifen (a control cancer drug) for comparison. Morphological study of the scaffolds was characterised with a scanning electron microscope. Drug release experiments and mechanisms of drug release (kinetics and order of drug release) were studied with ultraviolet visible spectrometer. Porosity of the samples were examined with ImageJ software. The inclusion of nanoparticles in the scaffold structure increased the pore size and pore diameter which also leads to the lowering the yield strength of the scaffold, while pore density and pore area enhanced drug diffusion from the scaffold matrix. Implications of the results were discussed for possible mechanical characterisation of scaffolds and cell viability studies using nanoparticles impregnated scaffolds.

Table of Content

List of Figures

List of Tables

Chapter One

1.0 Introduction

1.1 Background and Introduction

World cancer incidence has been projected to increase by 50 % (from 14 million to 21 million) from the year 2012 to 2030 [1]. It was also reported that, global cancer deaths are projected to increase by 60 % (from 8 million to 13 million) by 2030 [1].

In a human body, cells naturally multiply and die on regular bases [2]. This self-destruction of cells when noting their deficiency or old age is termed as *apoptosis* [3,4]. This regular and normal division of cells is scientifically termed as *mitosis* [2]. Sometimes, genes undergo an abnormal change or mutation [5]. Since the genes are part of the cell's 'brain' (nucleus), an abnormal change to the genes could possibly lead to an abnormal rate at which cells divide [5]. In most cases, these defective cells divide more rapidly and die less frequently as compared to the normal cells [5,6,7]. This rapid division of cells causes the establishment of a lump, commonly known as a tumour [5,6,7]. For the tumour to survive, it forms blood vessels that acts as an avenue for oxygen and nutrients, for its survival and growth [6]. This phenomenon is known as *metastasis*, describing the invasive nature of cells, especially cancerous cells [8] (Fig. 1.1).

What makes cancer lethal is when these tumours begin to interfere with the vital body organs [6]. Among the commonly interfered vital organs are the lungs, the breasts, the brain, the stomach, and more [7]. Early detection is key to positive outcomes. However, treatment almost becomes impossible when cancer gets to stage four, where it spreads to all parts of the body [7].

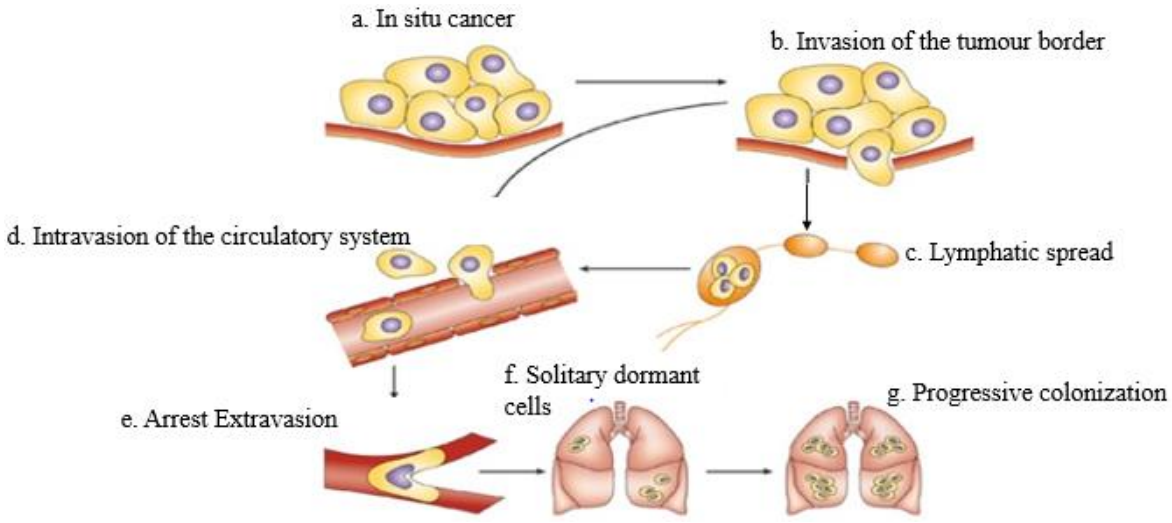

Figure 1.1: *Metastasis, and the Invasive Nature of Cancerous Cells.*

1.2 Problem Identification

Currently, the conventional cancer treatment methods include surgery, bulk systemic chemotherapy, and targeted therapy [8]. Surgery is the removal of cancerous cells or tumour through incision, laser, or low temperature cases [8]. However, surgery does not guarantee the removal of residual cancerous cells. Hence, the remaining cancerous cells later develops into tumours that may require post treatment surgeries [6,8]. Due to the aggressive nature of cancer, toxic drugs are administered during chemotherapy to stop or slow down the growth of cancerous cells [8]. However, chemotherapy is generally non-targeted and therefore affects any rapidly dividing cells, such as hair cells [8]. Destruction of normal cells therefore leads to malfunctioning of body organs [9].

Targeted therapy is a treatment method that seeks to target the nature by which cancerous cells divide and spread. Targeted therapy therefore uses small-molecule drugs to counterattack cancerous cells [8]. However, cancerous cells soon develop resistance to targeted medicine in this approach [8].

Most of the conventional treatment methods lack site targeting and specificity. Localized drug delivery has been highly studied in recent times for cancer treatment [9,10]. Thus, localized drug delivery could target the tissue sites specifically, while avoiding the exposure of non-target tissues/cells to toxic drugs. The current work is aimed at employing a nanoparticle-based 3D scaffold with desirable mechanical degradation, and drug release mechanisms for targeted cancer treatment [9,10,14]. This approach would ensure that scaffolds subsequently degrades by the natural metabolic activities.

1.3 Motivation and Justification

The birth of tissue engineering has somewhat been a beneficial substitute to tissue grafting and alloplastic tissue repair due to challenges like bio-incompatibility and donor unavailability [11, 14]. Tissue engineering has made it possible for the use of highly porous biodegradable scaffold biomaterials as dependable avenues for the regeneration of tissues [11,12].

Biological scaffolds are biologically engineered, temporary, artificial extracellular matrices essential for the regeneration of 3D functional tissues for medical purpose [25,26]. The common polymer used in making medical scaffolds is polylactic acid (PLA) which degrades in the human body releasing lactic acid (harmlessly released to the body) [26]. However, recent studies have displayed the possibility of combining PLA with polyethylene glycol (PEG), or PLA with poly-glycolic acid (PGA), making the composite structures more hydrophilic and biocompatible [26]. These structures (scaffolds) ought to possess several characteristics depending on their functionalities. These characteristics involve ‘appropriate’ biocompatibility, biodegradability, pore density and pore structure, mechanical capability, and reproducibility [26]. In recent times,

scaffolds do not only serve as avenue for tissue regeneration, but also as avenues for drugs release to vigorously counterattack any abnormality such as cancer [9,10,14].

Studies have shown that under proper constructive mechanisms (such as solvent casting), 3D scaffold can be an avenue for cell seeding that can lead to tissue regeneration [13]. The novelty of this project lies in the possibility of combining laser ablation and localized drug delivery with nanocomposite-based scaffolds with tuneable biodegradation, biocompatibility, and porous structures to mitigate potential side effects associated with the current conventional cancer treatment [9,10].

1.4 Objectives and Expected Outcome

The expected outcome of this project is to develop a nanoparticle-based solvent cast 3D scaffolds with significant pore structures as well as mechanical capability to enhance localized heating and controlled cancer drug release.

This outcome will be validated through series of objectives:

- Highly porous 3D nanoparticle-based scaffolds will be fabricated with poly-lactide-acid-co-poly-ethylene-glycol (PLA-PEG) through solvent casting techniques.
- Optical characterization of the 3D Scaffolds using scanning electron microscope (SEM).
- The porosity of the scaffolds would be well characterized: pore sizes, pore densities and pore distribution would be analysed with ImageJ software.
- Drug encapsulated scaffolds will be studied for the kinetics of the cancer drug release.
- SolidWorks would be used to mechanically simulate the static conditions of the scaffold in terms of deformation.

Chapter Two

2.0 Literature Review

2.1 Statistics on Cancer

According to the World Health Organisation (WHO), cancer is the second leading cause of deaths in the world, causing over 9.6 million deaths in 2018 (out of every 6 deaths, 1 is caused by cancer) [1]. The leading cause of deaths globally is cardiovascular diseases [39]. In 2018, lung cancer was recorded to have the highest mortality rate among other cancer types, followed by colorectal, stomach, liver and breast cancer [1,5,39]. The type of cancer with the highest incidence rate is lung cancer alongside breast cancer, followed by colorectal, prostate, stomach, and liver cancer [39]. Studies have shown that cancer is mainly caused by the following: high body mass index, low fruits and vegetables intake, lack of physical action or exercise and excessive use of tobacco and alcohol [5].

The WHO further points out that 70 % of the cancer-caused deaths occurred in the middle- and low-income countries, where the key cause of this huge number is the late-stage presentation and inaccessibility of diagnosis and treatments [5]. It was reported that there were over 90 % of treatment services available in high-income countries and less than 30 % available treatment services in the low-income countries [1].

2.2 Possible Cancer Interventions

Cancer interventions or treatment methods are categorized into three objectives: Primary treatment, Adjuvant treatment and Palliative treatment [17]. A cancer treatment method is prescribed based on the overall health of the patient, type of cancer or the stage in which the cancer is discovered [17].

The aim of primary treatment is to remove the tumour from patient's body or aggressively kill the cancerous cells [17]. Any cancer treatment can be used for this objective depending on the responsiveness or nature of the cancer being dealt with [17]. However, a common primary treatment is oncological surgery [17]. Oncological surgery removes the cancer or much of the cancer [8,17]. Oncological surgery is applied in the case of a tumour causing tremendous pain or pressure [17]. Despite this intervention, oncological surgery is limited to solid tumours situated at one place thus treatment against spread-out cancer will be impossible to be eliminated with this method alone [8,17]. Other treatment methods are then incorporated [17].

The aim of adjuvant treatment is to kill any leftover cancer cells after the primary treatment is done. Adjuvant treatment is a supplement to the primary objective of cancer treatments [17]. A common adjuvant treatment is chemotherapy [18]. Chemotherapy involves the administering of aggressively toxic drugs into the patient's body for the aim of preventing cancerous cells division, elimination of cancerous cells 'food' generators (enzymes and hormones) or directly killing cancerous cells [18].

Radiotherapy is another adjuvant treatment method [17,19]. This cancer treatment method involves the use of high energy particles such as X-Rays, electron beams, gamma rays to attack cancerous cells deposited in a specific region in the body [19]. Radiotherapy does affect nearby healthy cells but not effective as chemotherapy does [19]. In most cases, normal cells recover from radiation effect and go back to their ordinary tasks [19]. Radiation attacks cancerous cells by initiating small breaks in their DNA which cause them to seize growth and mitosis hence death of the cells occurs [19].

Palliative cancer treatments aim at relieving side effects during cancer treatments [17]. These treatments can include one or a summation of several cancer treatment methods [17]. An example

of a palliative cancer treatment is hyperthermia [20]. By incorporating hyperthermia to radioactivity, cancer treatment specificity will improve. Hence, healthy tissues will not be as affected as compared to radioactivity functioning on its own [20]. Apart from its palliative role, hyperthermia can take up a primary role. Hyperthermia involves subjecting the tumour to temperature of about 43^{o}C to 45^{o}C which kills tumour cells or make them more responsive to radiotherapy [21]. Example of these tumours are breast cancer tumours and melanoma tumours mostly found on the surface of the body [21]. Hyperthermia also assists in the easy diffusion of chemotherapy drugs [21].

2.3 Unresolved Issues

This section involves a discussion on some of the side effects and issues presented by the conventional cancer treatments methods.

2.3.1 Lack of Site Targeting and Specificity

One unresolved issue with the available cancer treatment methods is the impossibility of scoping out the impact unleashed onto the body by these treatment methods [8]. Most cancer treatment methods are invasive and do not only target cancerous cells but also nearby healthy cells [8,9]. There is a lack of site targeting and specificity in the conventional treatments available [8]. Bulk systemic chemotherapy tends to expose the entire body to toxic drugs [18]. In other words, it involves the administering of toxic drugs that aggressively attack rapidly dividing cells including but not limited to cancerous cells [18]. This means any rapidly dividing cells will be exposed to the gruesome effect of these drugs [8,18]. Cells that often encounter these drugs include white blood cells. This means during chemotherapy, there would be a loss of white blood cells. With the

decrease of white blood cells, the body has less potential to fight infections that regularly attack it. Apart from the loss of the general degree of the body immunity, chemotherapy can cause the loss of hair. This hair loss occurs in the head, breast areas for women, eye lashes, eye lids, pubic areas, arm pits, including the legs depending on the harshness of the type of chemotherapy drug used [22, 24]. Hair follicles are part of the rapidly dividing body cells which means toxic chemo drugs attack them as well [22, 24].

2.3.2 Recurrence of cancer

Recurrence of cancer refers to the revival of cancer in a local, nearby, or distant region of the body [23]. This occurs due to the breaking away of a tumour and its reestablishment in another area [23]. It can also be caused by the failure of oncological surgery to perfectly remove the cancerous cells from the region in which the tumour was removed [8,17,23]. It can also be caused by the dormant nature of some types of cancer [23]. But after an activity trigger, the cancer begins to vigorously divide [23].

Among the factors that would lead to a high recurrence probability of a cancer type include larger tumour size, lack of radiation after removal of cancerous cell, and cancerous cells that easily mutate making them resistant to adjuvant treatment [23]. The use of multiple cancer treatment methods has been employed to respond to the recurrent nature of cancer [23].

2.4 Engineered Scaffolds and Tissue Regeneration

With the inevitable recurrence of diseases, injuries, and trauma, it has become immensely necessary to invest expertise in the field of tissue repair, replacement, or regeneration [27]. An old means of treatment is an autograph and an allograph [27]. An autograph is the transfer of tissue

from one site to the diseased or injured site within the same body [11,27]. An allograph is a transfer of tissue from one body to another injured or diseased body. Despite the significant aid that these treatment methods have offered, limitations are inescapable. Autographs are profoundly painful, expensive, and susceptible to donor-site morbidity [11,14,27]. Allographs are challenged by the scarcity of enough tissues to serve the needs of the numerous tissue-replacement-demanding patients. Aside that challenge, there is a fear of tissue rejection by the immune system of the patient as well as a possibility of introducing infections or diseases into the receiving body [14,27].

A rapidly growing field of study is tissue regeneration [11,12]. Tissue regeneration is a supported renewal and growth of a tissue on the diseased or injured site. This regeneration is made possible through combining health body cells with a highly porous scaffold biomaterial [11,12]. Under conducive biochemical and physio-chemical factors, this highly porous scaffold biomaterial will guide the growth of new tissue [11,12,13] (Fig. 2.1). Regardless of the type of tissue to be regenerated, when designing the highly porous scaffold biomaterial several requirements must be considered: biocompatibility, biodegradability, mechanical properties, scaffold architecture and manufacturing technology [25,26].

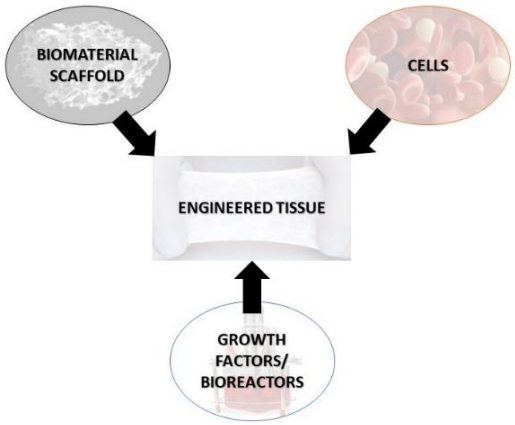

Figure 2.1: *An illustration of the necessities involved in engineering a tissue.*

2.5 Biopolymers for scaffold design

Biopolymers are polymers originating from living organisms. Like all polymers, monomers covalently bond onto one another forming a chain-like structure called a polymer [28]. Among the well-known polymers include polylactic-co-glycolic (PLGA), poly(ε-caprolactone), polylactic acid (PLA), poly(3-hydroxybutyrate-co-3-hydroxyvalerate), chitosan and more. [28] (Table 2.1).

Aside their abundancy and unique biological characteristics, biopolymers are also biocompatible [29]. This means they can effectively work in contact or in close vicinity to the body and bodily fluids without altering the normal functions or triggering any side effect or allergic reactions. It is their biocompatibility factor that has provided basis for intense use in the biomedical field (Table 2.2). Biopolymers are used in tissue scaffolding, artificial grafting, controlled drug delivery, as a bone filler material, and implantation [30].

Table 2.1: *Classification of well-known biopolymers.*

Biodegradable				**Nonbiodegradable**
Bio-Based			***Fossil-Based***	***Bio-Based***
Plants	*Microorganisms*	*Animals*		
Cellulose and its derivatives (polysaccharides)	PHAs	Chitin (polysaccharides)	Poly(alkylene dicarboxylate)s e.g. PEA, PPF, PTT, etc.	PE (LDPE, HDPE), PP, PVC
Lignin	PHF	Chitosan (polysaccharides)	PGA	PET, PPT
Starch and its derivatives (monosaccharides)	Bacterial cellulose	Hyaluronan (polysaccharides)	PCL	PU
Alginate(polysaccharides)	Hyaluronan (polysaccharides)	Casein (protein)	PVOH	PC
PLA (from starch or sugar cane)		Leather (protein)		Epoxy

[PE] Polyethylene, [LDPE] Low density polyethylene, [HDPE] High density polyethylene, [PP] Polypropylene, [PVC] Polyvinyl chloride, [PHA] Polyhydroxyalkanoates, [PHF] Poly-1-hydroxymethylethylene hydroxymethyl-formal, [PEA] Poly(ethylene adipate), [PPF] Poly(Propylene Fumarate), [PTT] Polytrimethylene terephthalate, [PGA] Poly(glycolic acid), [PCL] Polycaprolactone, [PVOH] Poly(vinyl

alcohol), PET Polyethylene terephthalate, PPT Polypropylene Terephthalate, PU Polyurethane, PC Polycarbonates.

Table 2.2: *Common polymers and their medical significance.*

S. No.	Polymers	Properties Suitable for Medical Applications	Applications
1	Polylactic Acid (PLA)	▪ PLA degrades within the body after incision has healed. ▪ Copolymers of PLA and PGA are more useful than homopolymers of PLA and PGA because their rate of degradation can be adjusted.	▪ Devices made of PLA-PGA copolymer have been used for the controlled release of antibiotics, anticancer and antimalarial agents, contraceptives, hormones, insulin, narcotic antagonists, and proteins
2	Polyglycolic Acid (PGA)	▪ Insoluble in water ▪ Biodegradable	▪ Suture (stitches holding together the edges of a wound or surgical incision) ▪ Drug delivery ▪ Tissue engineering
3	Poly(lactic-co-glycolic) acid (PLGA)	▪ Tailored biodegradation rate (depending on the molecular weight and copolymer ratio) ▪ Potential to modify surface properties to provide better interaction with biological material ▪ Degrades rapidly than PGA and PLA	▪ Ligament/Tendon repair ▪ Biodegradable Stents ▪ Bone fixation devices

2.6 Nanoparticles-based Scaffolds

Nanoparticles are particles with dimensions measured in nanometres (nm; 1 nm = 10^{-9} m). Nanoparticles can naturally be found in the world and also can be produced through everyday human activities. Due to their uniquely small size, nanoparticles can have unique material properties [31].

Nanomedicine, a branch of nanotechnology, has recently been highly beneficial especially in the tissue regeneration field. Nanoparticles run from being used as drug delivery vessels in porous biodegradable scaffolds, to being used as an enhancive entity in targeted cancer treatment (Photothermal therapy) [32]. According to Sahai et al., "Nanomedicines are used to bind/encapsulate in porous biodegradable scaffolds in the form of antibiotics, proteins, growth factors, specific micro- and macro-nutrients to promote tissue regeneration." [33].

It has been scientifically proven that when cancerous cells are subjected to temperature ranging from 43^{o}C to 45^{o}C, the cells undergo programmed cell death [34]. Nanoparticles are essential in raising up the cellular temperatures to that range hence performing targeted cancer treatment [34].

2.7 Laser Ablation and Localized Cancer Treatment

Laser ablation is generally a process of focusing an energetic laser beam onto an area for the goal of removing or killing materials in the irradiated region [35]. It is also referred to photoablation [36]. It involved the use of heat produced from light rays' concentration to remove undesired material from the irradiated region [36].

According to Schena et al (2017), laser ablation is done using a laser beam which transports the laser light into the tissue at a specific wavelength. The wavelength defines the properties of the laser and the interaction with biological tissue [37]. Laser ablation could be involved in localized treatment of cancer [37]. It eradicates cancer tumours without removing them [38]. Laser ablation subjects a tumour with appropriate temperature that will initiate cancerous cells' death [34,38]. Laser ablation is often used for small localized tumours in place of surgery.

2.8 Scope of Project

The first chapter presented the background studies on the subject area. The problem statement, motivation, goal, and objectives as well as expected outcomes were clearly highlighted in chapter one.

Extensive literature survey was presented in the second chapter of this report. Statistics on cancer incidence and mortality rates were presented. Moreover, the current conventional methods of cancer treatment were present with their challenges for future directions. Review on biopolymers and nanocomposite scaffolds were also presented for the design of tissue engineered scaffolds to serve as alternative treatment modalities for cancer treatment.

Moreover, the third chapter presents the design, materials, and methods. The design covers the requirements and materials selection. Methodologies comprised of experimental procedures, computational simulation and different materials characterization and techniques. Examples of test cases include, but not limited to, determining the effect of porogen on the porosity of PLA-PEG, effect of nanoparticles on PLA-PEG, effect of drugs release on PLA-PEG scaffold. Also, mechanical characterization include tensile and compressive strength.

The fourth chapter presents a section on the analysis, results, and scientific discussions. Implications of the results are then discussed for the development of potential cancer treatment with nanocomposite scaffolds.

The fifth chapter presents the concluding remarks, recommendations, limitation, and suggestions for future works related to the project.

Chapter Three

3.0 Materials and Methods

3.1 Design Requirements

The design requirements are summarized in Table 3.1.

Table 3.1: *Table showing design requirements and indicative remarks.*

Design requirement	**Meaning**
Biocompatibility	Device should be able to support cellular activities as an attempt to regenerate a new tissue, without bringing harm to the host tissue.
Biochemical Degradation	Device should be able to indicate mass loss as a sign of biodegradation over time.
Porosity	Device should support the presence and appropriate distribution of pores essential for cell seeding and tissue regeneration.
Geometry	Device should be able to cover the entire affected area that will encounter laser ablation and guide the tissue regeneration.
Mechanical performance	Device should have sufficient potential to withstand the dynamic mechanical reality of the human body.
Drug release mechanism	Device should be able to periodically(controllably) release drugs that would kill any residual cancerous cells immediately, and progressively after the laser ablation procedure.

3.2 List of Materials

Cancer drugs: Tamoxifen (control drug), Dichapetalin M (Dic M) (experimental drug) were supplied by the Biochemistry and Chemistry Department, The University of Ghana. Magnetite, gold nanoparticles and polyvinylpyrrolidone (PVP) were supplied by Dr. Danyuo Yiporo at Ashesi University, poly-ethylene glycol (PEG) was procured at a chemical shop in Accra, while poly-lactic-acid (PLA) filament was supplied by the mechanical lab at Ashesi University. Porogen (salt), distilled water, ethanol, acetone, di-chloro-methane, falcon tubes (15 ml and 50 ml), and other consumables were procured from a chemical shop in Accra. Lastly, surface-treated tissue culture plate (6/12-wells plates) were procured from Life Science Plasticware (Illinois, USA).

3.3 Experimental Design and Procedures

3.3.1 Solvent casting

Solvent casting process involves the solidification of poly-lactic-acid-co-poly-ethylene-glycol polymer through the escape of a highly volatile organic solvent from the mixture. PLA filament was cut into pellets (1 cm rods) and weighted according to experimental design (Table 3.2) using an Analytical balance (Mettler Toledo®, ME 103, Columbus, Ohio, USA). An organic solvent, dichloromethane (DCM) was used to melt the polymers (PLA and PEG) at $90℃ - 100℃$ in an airtight glass container (to prevent DCM from escaping). Physical process with stirring was done at regular interval to ensure a homogenous polymer solution were obtained. The polymer solutions were left at room temperature for 24 h to enable all particles within the solution to dissolve. Control scaffold comprised of PLA, cast in circular mini glass petri dishes (diameter = 30 mm), while the porogen (95% of polymer mass) was sprinkled onto the cast polymer immediately. The density of the salt allows it to slowly fall through the molten polymer.

However, PVP was then added to the magnetite nanoparticles (Fe_3O_4) and dissolved with DCM. The PVP- Fe_3O_4 solution was then introduced to designed sample codes C-E (Table 3.2). About 95 % of grinded salt particulates were introduced to sample codes A-E as porogen to enhance the porosity of the scaffolds. A volume of 4 mL of cancer drugs were introduced into sample codes A, B, C and E to study the effect of Tamoxifen and Dic. M on the microstructure of the scaffolds. Drug loaded scaffolds were subsequently used for drug release kinetics and for the study of cell viability in the future. Samples were then cast and allowed to dry in an open (at room temperature). The volatility of the DCM enhances its evaporation from the scaffold after casting. The illustration in Figure 3.1 showed the solvent casting process. Leaching was then carried out after 24 h of casting. Samples were saturated with 500 ml of distilled water inside glass beakers. Fresh distilled water was replaced at 12 hr interval for about 5 days to ensure the salt (porogen) has dissolved and leached out. Experimental scaffolds were placed on filtered papers and dried at laboratory temperature. Scaffolds at this stage were then ready for drug release experiments, optical characterization, and mechanical testing.

Table 3.2: *Table showing sample cases and measurements needed.*

Sample Code	**PLA**		**PEG**		**Fe_3O_4 nano-powder**	**Cancer Drugs (4 mL)**		**Grinded Table Salt (NaCl as porogen)**
	%	Mass (g)	%	Mass (g)	5% of Polymer Mass (0.750 g)	Tamoxifen	Dic M	95% of polymer mass (14.250g)
Control	100	15.0						
Sample A	80	12.0	20	3.0		✓		✓
Sample B	80	12.0	20	3.0			✓	✓
Sample C	80	12.0	20	3.0	✓	✓		✓
Sample D	80	12.0	20	3.0	✓			✓

Sample E	80	12.0	20	3.0	✓		✓	✓

✓ The presence of that entity in the respective sample code: ^{Tamoxifen} Control Drug, $^{Dic\ M}$ Dichapetalin M (Experimental Drug), ^{PLA} Poly-lactic-acid, ^{PEG} Poly-Ethylene-Glycol.

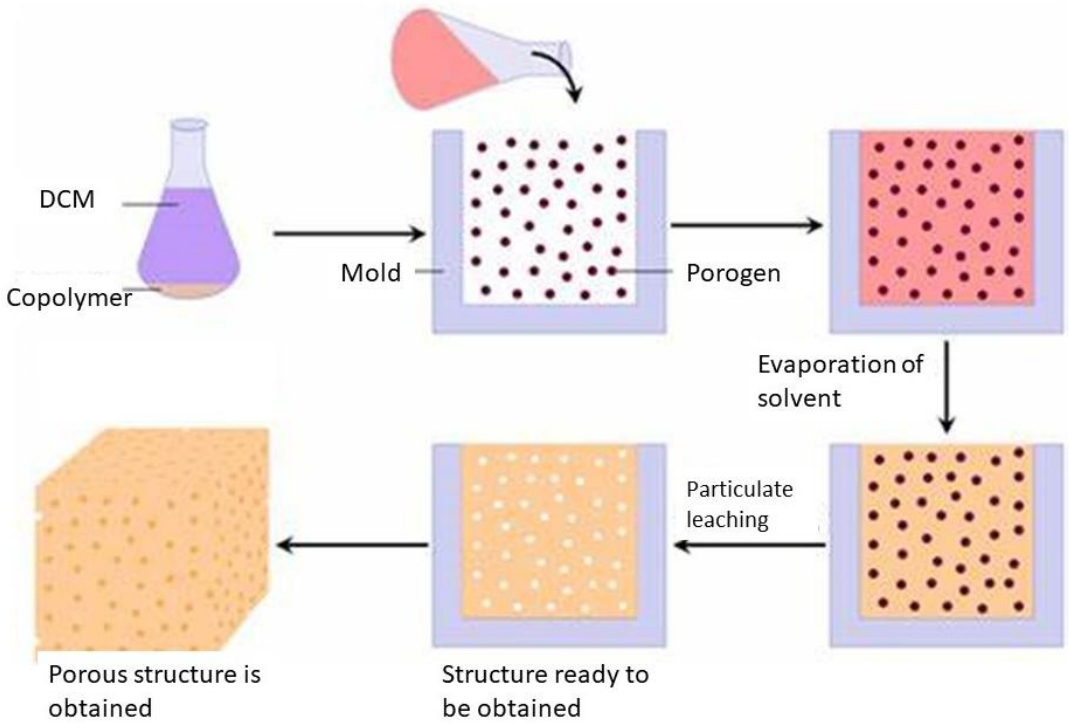

Figure 3.1: *An image-flow portraying solvent casting and particulate leaching processes.*

3.3.2 Kinetics of the Cancer Drug Release

The study of cancer drug release would require biological fluids. In view of this, phosphate buffer saline (PBS) solution was prepared at pH 7.4 to simulation physiological conditions. Initial absorbance of the prepared drug solution was obtained using an ultraviolet visible spectrophotometer (Jenway Genova Bio Spectrophotometer, 720601, Jenway, Cole-Parmer Ltd Stone Staffordshire, ST15 0SA, United Kingdom). Drug release was done in triplicates. Sections of PLA-PEG were cut and placed into falcon tubes filled with 4 ml of pH 7.4 PBS using 5 ml Euro-

Ject-III single use syringes. Drug release was done at 37 ℃ inside an orbital incubator shaker set at 60 rpm (Incu-shaker Mini, H1001-M, 2600 Main Street Extensions, NJ, USA). Absorbances were recorded at peak value at specific wavelengths for both drugs and converted to concentration of drug release as a function of time. Samples after the UV-vis measurements were stored in a ULab 1.5 ml microcentrifuge tube in a deep freezer for future use. Drug release was guided by Beer-Lambert Law:

Beer Lambert Law is mathematically expressed over the visible range of light absorption in the sample at known wavelengths given by:

$$\boldsymbol{A(\lambda) = e(\lambda)\, l\, c} \tag{3.1}$$

where A(λ) is the Absorbance, e(λ) is the molar absorptivity constant which changes dependent on wavelength (250-400 nm), l is the path length (cross-section of cuvette through which light travel through the liquid), and c is the concentration of solution. Figures 3.2a and 3.2b are the pictures of the Jenway Genova Bio Spectrophotometer and Incu-shaker Mini, respectively.

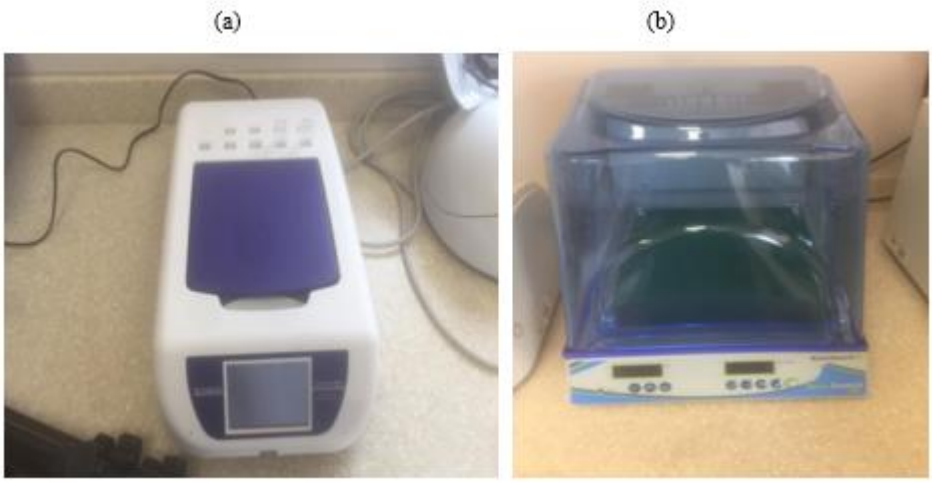

Figure 3.2: *(a) Jenway Genova Bio Spectrophotometer (b) Incu-shaker Mini.*

3.3.3 Investigating the order of drug release

Investigation on the order of drug release was performed by making use of rate laws and graphical models. The order of drug release is basically a study of how the rate of drug release is affected by the progressive fall in concentration of the drug. The orders of drug release were investigated through the following equation (3.2):

$$\boldsymbol{R = k[C]^n} \qquad (3.2)$$

where R is the rate of concentration fall, k is the rate constant, C is the concentration and n is the order of release. For zero order n = 0, for first order n = 1 and for second order n = 2.

To test whether a set of experimental data abides to the first order of release, a graph of the natural log of concentration against time was plotted. If the resultant graph is a negative slope straight line, then the set of experimental data is that of first order. To test whether a set of experimental data abides to the second order of release, the first order test is performed, which will result into a curve. After that test, a graph of the inverse of concentration against time is plotted. If the resultant graph is a positive slope straight line, then the graph is a second order graph. The kinetics models including zero order, first order, second order and Huguchi were used to examine the rate of drug release from the polymeric matrices. The linear relations of the model equations are summarized in Table 3.3:

Table 3.3: *Linear Relations of the Model Equations [40].*

Model	Equation
Zero-order	$C_t = C_o + k_o t$
First-order	$lnC_t = lnC_o + k_o t$
Second-order	$\frac{1}{C_t} = \frac{1}{C_o} + k_o t$
Higuchi	$C_t = C_o + k_o t^{\frac{1}{2}}$

where k_o is the rate constant for the given model, C_t is the concentration at time t, and C_o is the initial concentration.

Higuchi model was discovered in 1961 by a legendary professor Takeru Higuchi [43]. This model basically explained the order or mechanism of drugs transportation in polymeric matrices. To test whether a drug abides to this model, concentration would be plotted against the square root of time. The resulting graph must be a positive slope straight line.

$$\mathbf{Q = k_o t^{1/2}} \tag{3.3}$$

where Q is the cancer drug concentration, k_o is the Higuchi constant, and $t^{1/2}$ is the square root of the time in hours.

To test the linearity of the resultant test graphs, the coefficient of determination (R^2) was used. The coefficient of determination is a statistical tool, ranging from 0-1 that allows us to measure the goodness of fit. The closer a graph's R^2 value is to 1, the better the graph's fit to a certain model.

Concentration versus time graphs of all samples would be passed through the three tests, then coefficients of determination (R^2) of each resultant model test graphs would be compared and the resultant test graph with the highest R^2 would inform us that a particular concentration versus time graph belongs to that model.

3.3.4 Optical Characterisation

Morphological characteristics of the microstructures of the scaffolds were investigated with Phenom scanning electron microscope (Phenom, Eindhoven, The Netherlands). Imaging was done at different resolutions. Porosity of the samples were subsequently done using ImageJ software (Wayne Rasband, University of Wisconsin-Madison, USA). Following the study of porosity, the samples were characterised to determine the pore sizes, pore densities and pore distribution.

3.3.5 Mechanical analysis with SOLIDWORKS

Figure 3.3 presents CAD models of PLA scaffold, PLA-PEG scaffold, and PLA-PEG-Nanoparticles scaffold (260.47 µm by 286.32 µm by 20 µm). The necessity to come up with these designs was for the goal of knowing how pore density and pore sizes affects the mechanical strength of the scaffold through the application of tension force.

The force applied was a product of the design yield strength and the perpendicular area of the surface where the force would be applied. The design yield strength was calculated from dividing the actual PLA yield strength with a safety factor of 3.5. The yield strength was 20 MPa, the tensile force applied on the scaffold was 0.00157 N and the compressive force was 0.44958 N. Tensile loading was done by applying force in opposite directions, while compressive forces were applied on the surface of the scaffolds (while the opposite face was statically fixed.

After obtaining the force values needed, a mesh was created (Fig. 3.4) for every CAD sample, and mechanical simulation were carried out.

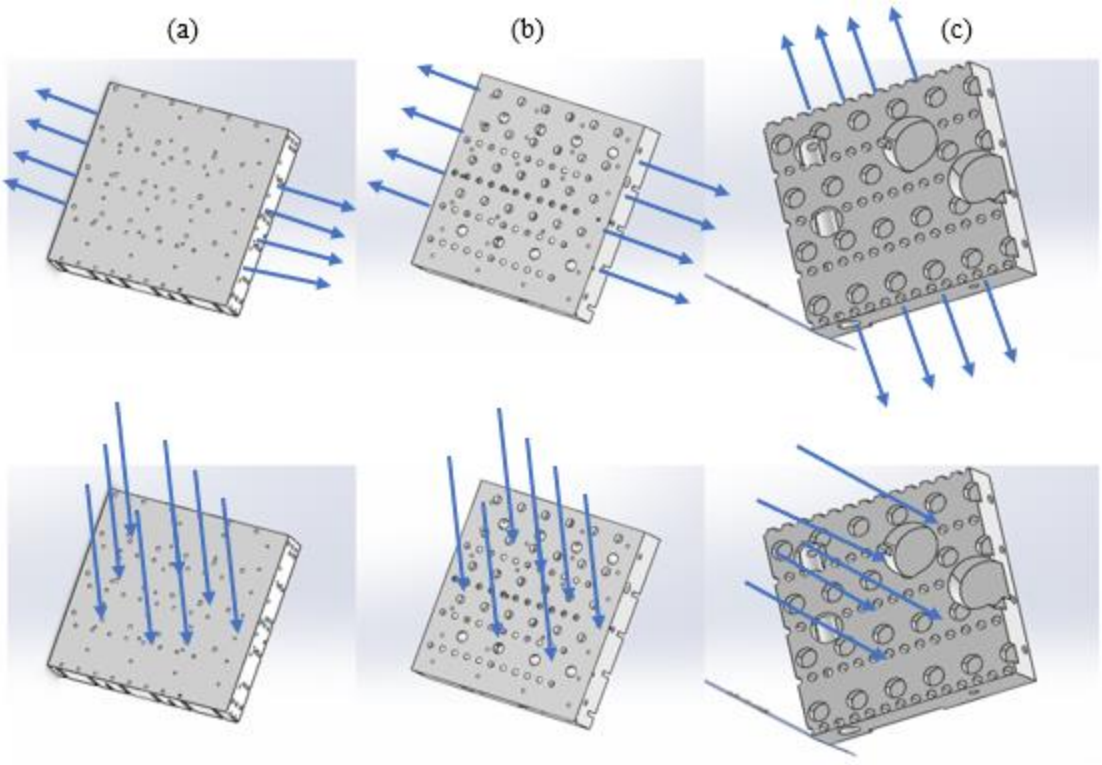

Figure 3.3: *CAD model of a piece of: (a) PLA scaffold, (b) PLA-PEG scaffold, and (c) PLA-PEG-Nanoparticles scaffold.*

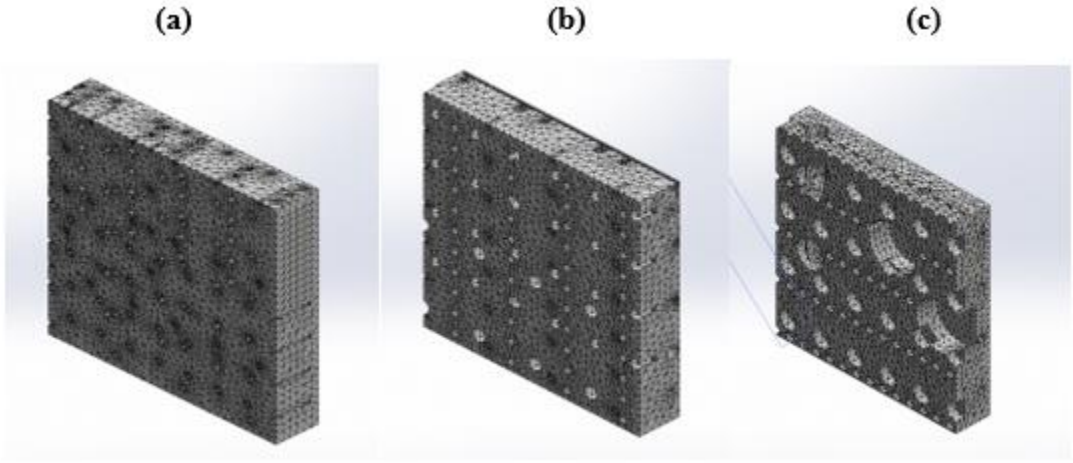

Figure 3.4: *Mesh images of:(a) PLA scaffold (b) PLA-PEG scaffold (c) PLA-PEG-Nanoparticles scaffolds.*

Chapter Four

4.0 Results, Analysis and Discussion

4.1 Morphological Analysis of the 3D Scaffolds

Figure 4.1 below is a collection of images displaying the resultant scaffolds after solvent casting and particulate leaching. One clear difference is the colour of samples that contain nanoparticles, from ones that did not contain nanoparticles. Scaffolds containing magnetite nanoparticles were darker due to the black colour of Iron (II,III) oxide, powder. Samples with porous with the presence of salt (as the porogen) and porosity was associated with rough surfaces especially when nanoparticles were incorporated.

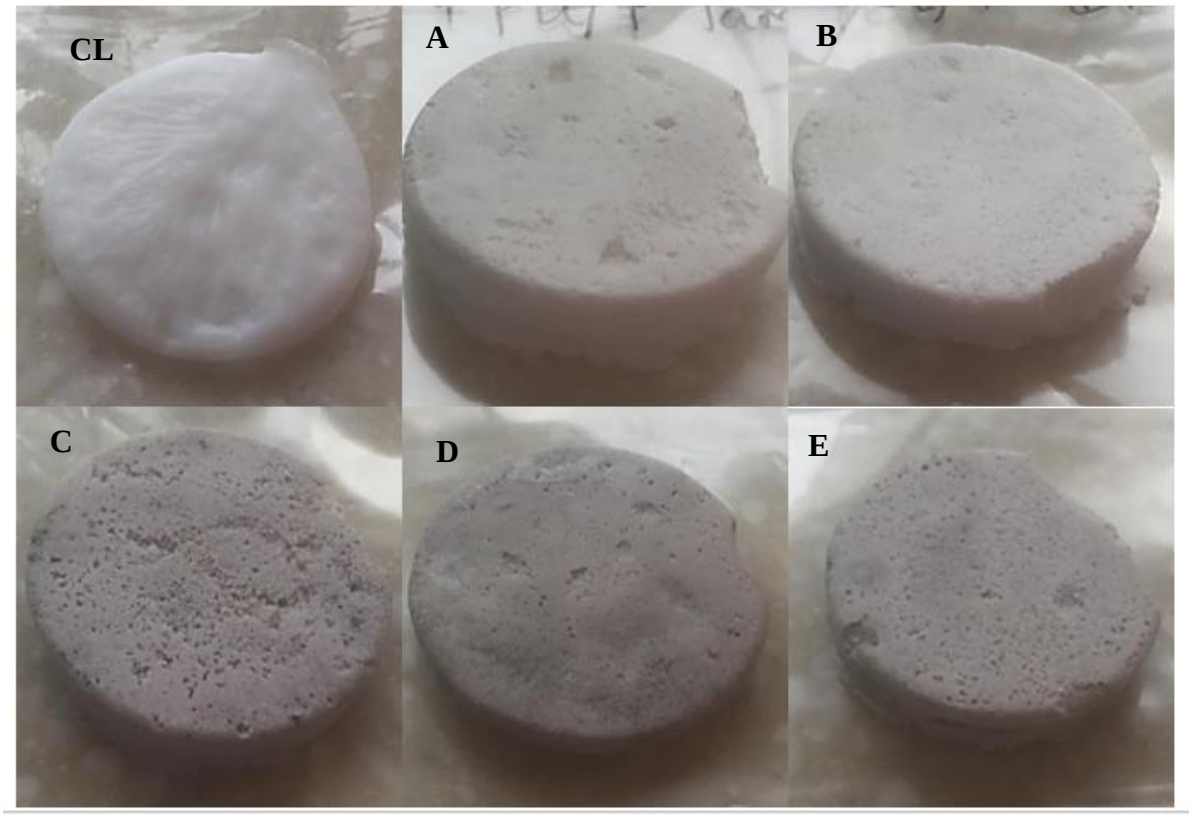

Figure 4.1: *From top left (to the right): Control (CL), Sample A, Sample B. From bottom Left (to the right): Sample C, Sample D, Sample E.*

Figure 4.2-I displays the microscopic images of three scaffolds. From the three images, it was observed that the scaffold sample with just PLA (Control sample) did not lack porosity (Fig. 4.2-Ia), despite the fact that no porogen was added. The presence of the micropores/macropores is because of the volatility of DCM which also act as a pore forming agent especially when it evaporates from the polymer matrix during solidification. A mean pore diameter of 4.897 μm per 50 pores were measured within the PLA sample. PEG is a hydrophilic polymer and its presence in PLA (PLA-co-PEG sample) (Fig. 4.2-Ib) helps to enhance the porosity of the scaffolds and the porosity becomes more pronounce when porogen such as salt particulates were introduced and leached out during casting. That is, PEG is a hydrophilic polymer which enhance the pore density of the scaffold. Also, leaching out the salt which acts as a porogen enhances the pore density of the scaffold which could enhance drug diffusion, cell seeding, and protein absorption. Thus, the water-soluble porogen (table salt) dissolved in the distilled water hence leaving a pit-like pore structure essential for proliferation/percolation of cells, air, or nutrients. However, the size of pores varies.

The effect of Iron (II,III) oxide powder (nanoparticles) played a vital role in increasing the pore sizes/pore area (Fig. 4.2-Ic). A mean pore diameter of 18.845 μm per 50 pores was reported for a scaffold that contained nanoparticles (Fig. 4.2-IIc). This result is almost twice the pore diameter of 8.823 μm per 50 pores that was measured for a PLA-PEG scaffold that lacks iron nanoparticles (Fig. 4.2-IIb).

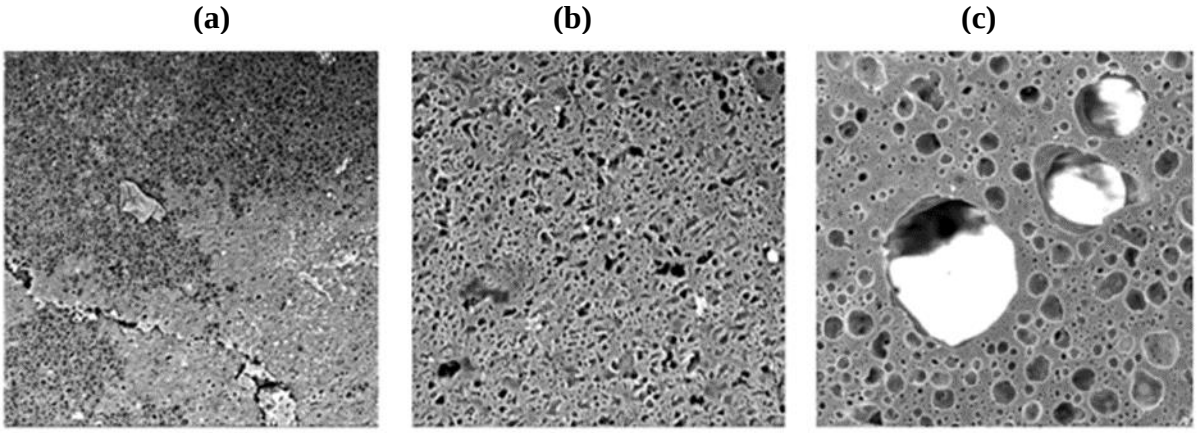

Figure 4.2-I: Scanning Electron Microscopy Images: (a) Morphology of PLA scaffold, (b) Morphology of PLA-PEG scaffold, (c) Morphology of PLA-PEG-Nanoparticles scaffold.

The pore sizes for the control sample ranges from 3-7 μm with dominance of 4.1-5.0 μm (representing 32%) (Fig. 4.2IIa). Pore size/pore area were found to increase from 3-17.4 μm for PLA-PEG sample containing a pore forming agents (Fig. 4.2IIb). Dominated pores for this sample was within the range of 7-10.12 μm (representing 42%) (Fig. 4.2IIb). Larger pore areas with less pore density were observed when PLA-PEG samples were loaded with magnetite nanoparticles (Fig. 4.2IIc). The dominance pores were within the range of 3.83-18.54 μm (representing 70 %) (Fig. 4.2IIc).

(a)

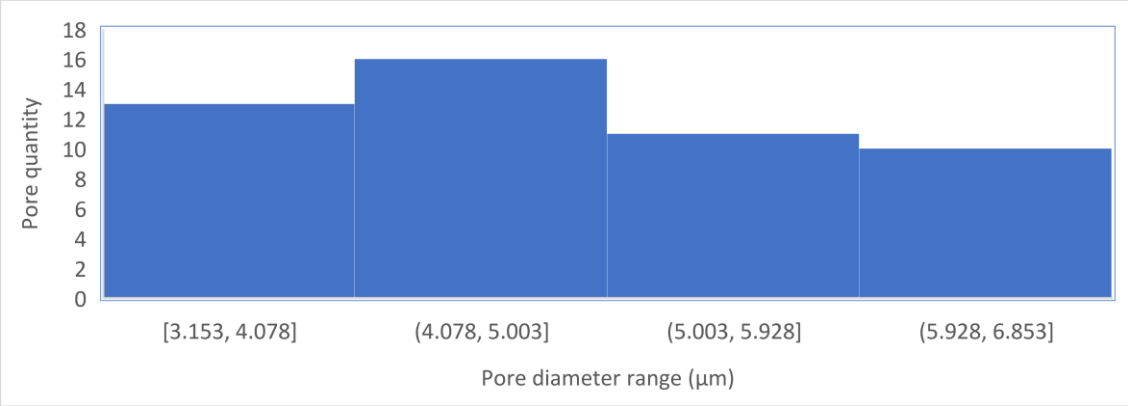

(b)

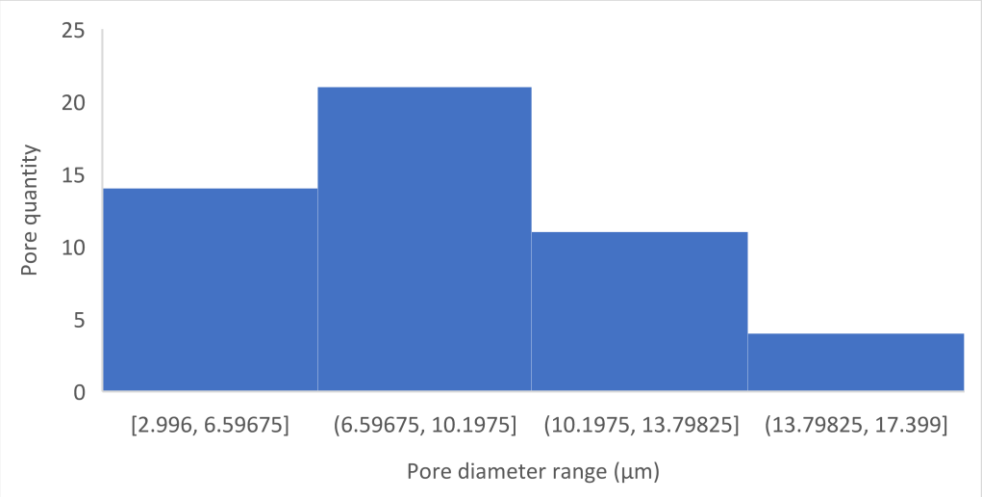

(c)

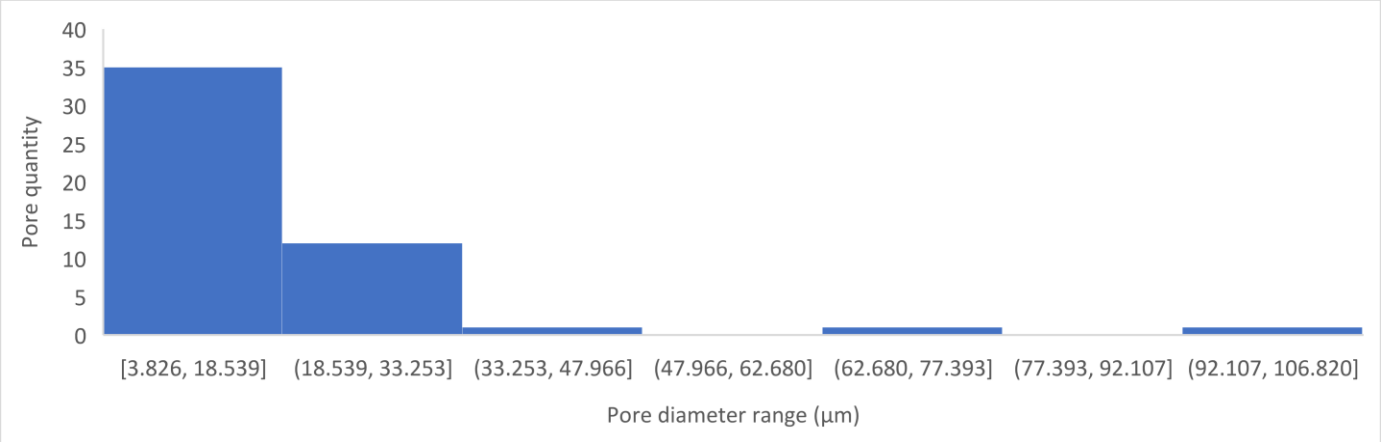

Figure 4.2-II: *Pore distribution of Scaffolds: (a PLA scaffold, (b) PLA-PEG Scaffold, and (c) PLA-PEG-Nanoparticles Scaffold.*

4.2 Kinetics of Cancer drug release

Figure 4.3 displays the relationship of absorbance against wavelength for the control drug (Tamoxifen drug) (Fig. 4.3a) and experimental drug (Dic M) (Fig. 4.3b). Figure 4.3a shows that the maximum absorbance for the Tamoxifen is 1.081 at a wavelength of 297 nm, while Dic M had a peak absorbance of 0.581 at a wavelength of 295 nm.

Standard curves, which depict the relationship between concentration and absorbance are presented (Fig. 4.4). Both graphs reveal a common trend of increase in concentration as absorbance increases. However, the release concentration and absorbance of Tamoxifen were higher than the Dic M (Fig. 4.4). The standard curves would help researchers working with tamoxifen and Dic M to easily interpolate with measured absorbance to determine a given concentration of drugs release.

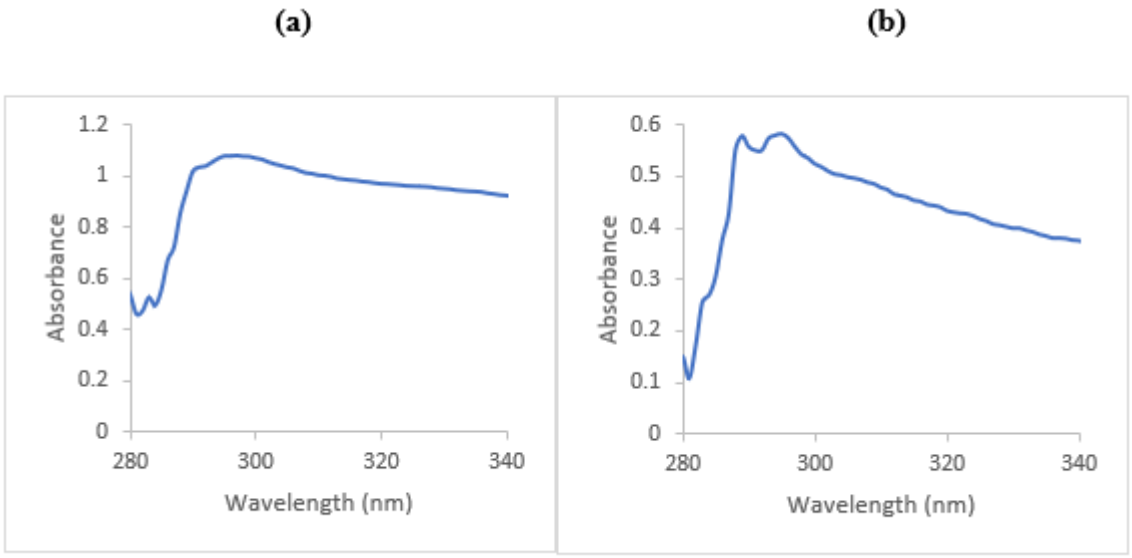

Figure 4.3: *Maximum Absorbances of Drugs: (a) Tamoxifen and (b) Dic M.*

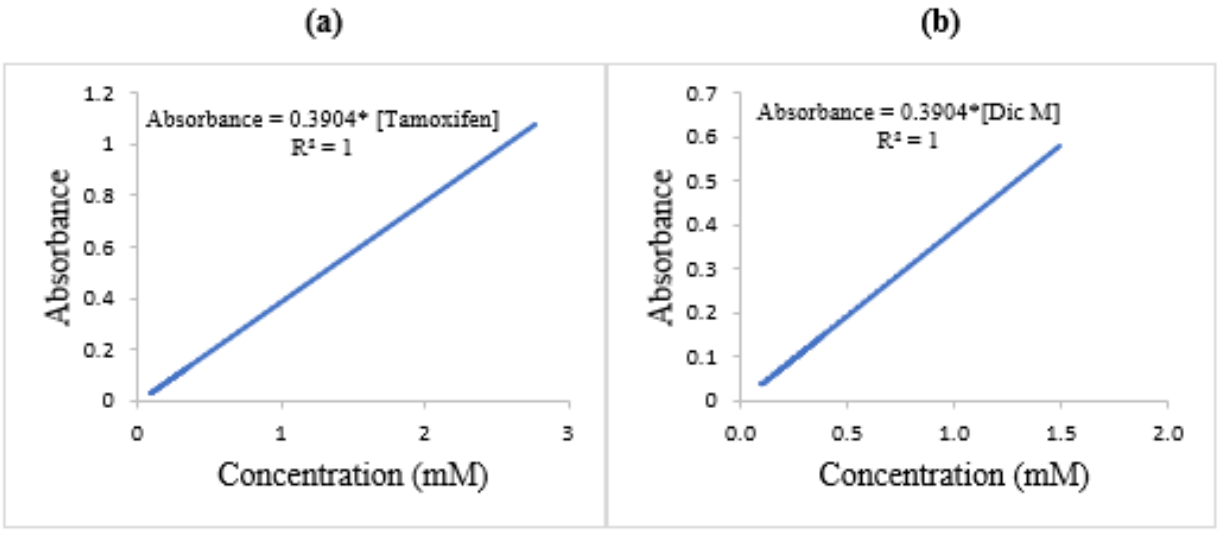

Figure 4.4: *Standard curves: (a) Tamoxifen and (b) Dic M.*

In terms of kinetics, the data (Fig. 4.5) shows an exponential fall in drug concentration with time. Drug release was higher within the first day but decreased exponentially with time. However, there was a transient decrease and sudden increase in drug release. Due to the mutable nature of cancerous cells, medical researchers have come into an awareness of coming up with cancer drugs that contain a sense of unpredictability. Thus, before the cancer cells gets accustomed to a certain manner of drug behaviour, a sudden change in the drug behaviour could occurs to keep up with the mutable cancer. This is good for treating and suppressing recurring diseases such as cancer [41].

(a)

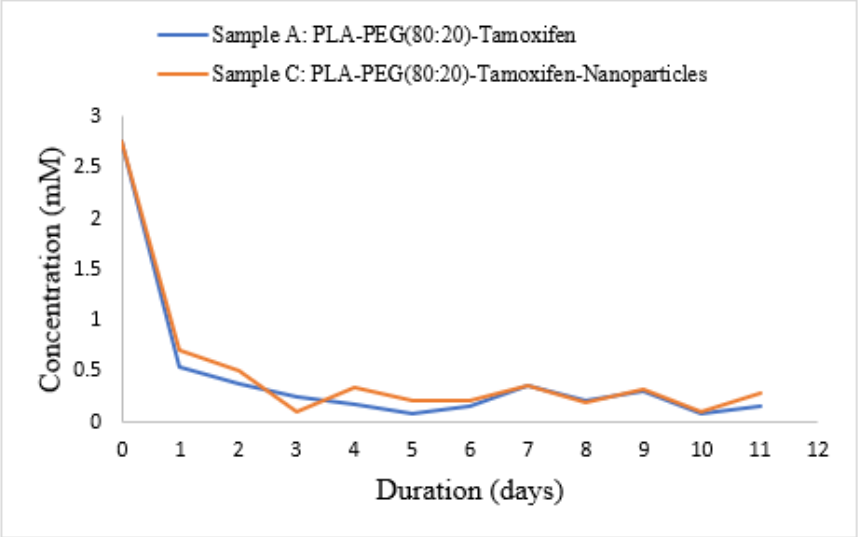

(b)

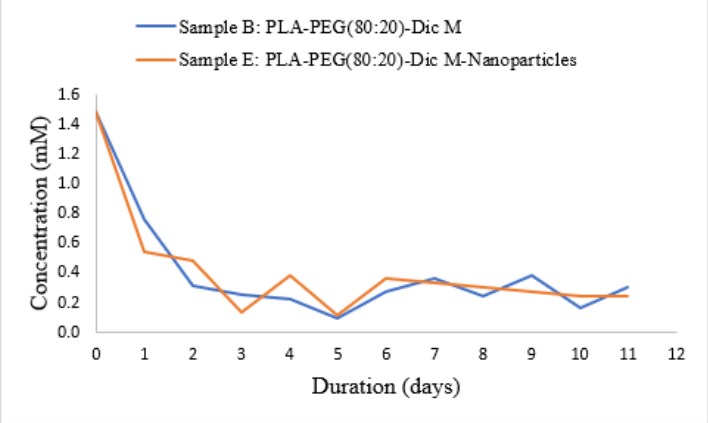

Figure 4.5: *Concentration Versus duration of drug release: (a)Tamoxifen-containing samples (b) Dic. M-containing samples.*

4.3 Order of drug release

For a graph that predicts the response variable (drug release) to acceptably exhibit a certain model of drug release, its R^2 value must be in the range 0.95 to 1[42].

From Table 4.1 and Table 4.2, we observe that both Tamoxifen and Dic M cancer drugs have low R^2 value. However, the Higuchi model is one with the highest R^2 value. One prediction is that, in

the abundance of more data, the graph might fully show a leaning towards Higuchi model of drug release (a model that is widely used in polymeric matrix systems) [43].

Table 4.1: *Comparison of R^2 values for Tamoxifen-containing samples.*

	R^2 VALUES		
	1st order model test	2nd order model test	Higuchi model test
Sample A: PLA-PEG(80:20)-Tamoxifen	0.4134	0.2787	0.5773
Sample C: PLA-PEG(80:20)-Tamoxifen-Nanoparticles	0.3434	0.1421	0.5991
R^2 value average	**0.3784**	**0.2104**	**0.5882**

Table 4.2: *Comparison of R^2 values for Tamoxifen-containing samples.*

	R^2 Values		
	1st order model test	2nd order model test	Higuchi model test
Sample B: PLA-PEG(80:20)-Dic M	0.2508	0.0851	0.5979
Sample E: PLA-PEG(80:20)-Dic M-Nanoparticles	0.2529	0.0623	0.6005
R^2 value average	**0.2519**	**0.0737**	**0.5992**

As a reminder, zero order of release means that the rate of drug release is not affected by the progressive fall in the concentration. In other words, the rate of the fall in concentration (drug release from the scaffold) is time in dependent [44] (Figure 4.6a). First order of release means that the rate of drug release falls due to the progressive fall in the concentration of the drug in the

scaffold [45]. In the first order of release, the rate of decrease in molar concentration depends on one reactant alone. The second order is a release in which the rate of drug release is dependent on the concentration of two reactants or the concentration of one reactant to the second power.

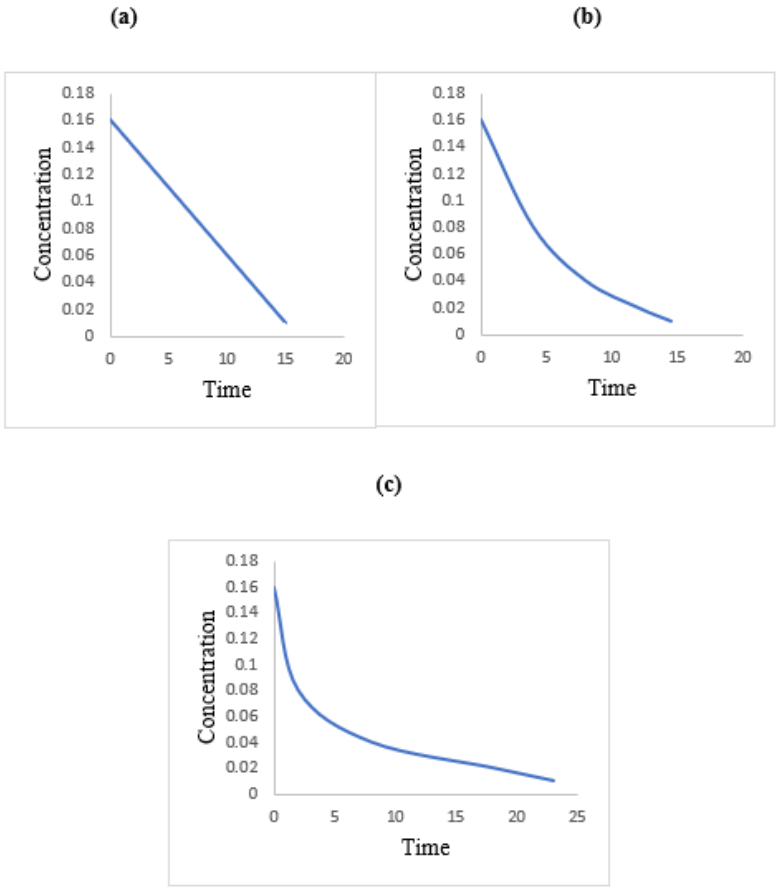

Figure 4.6: *Order of Drug Release and Drug Release Mechanism: (a) Zero Order, (b) First Order, (c) Second Order or Higuchi*

4.4 Mechanical analysis with SolidWorks

From the mechanical simulation of the three scaffold CAD models, displacements (deformation), stress and strain are shown in Figures 4.7 and 4.8. When tension and compressive forces are applied, the least displacement was experienced by the PLA sample, whereas the highest displacement was experienced by the PLA-PEG-Nanoparticles sample. This implies that the

increase in pore density and diameter plays a significant role in the strength of the scaffold. This also means the modulus or perhaps the hardness of the scaffold will be reduced with pore density and the presence of PEG and nanoparticles in the scaffolds since deformation was more pronounced in axial loading. This in a way will ensure that, the properties of the scaffolds are lowered to match with the mechanical properties of normal tissues. Generally, compressive strength was higher than the tensile results. Compressive strength closes microcracks/microvoids, which tensile test opens this pre-existing cracks/voids. Hence, the structure will resist more loads in compression than in tension as shown in Tables 4.3 and 4.4.

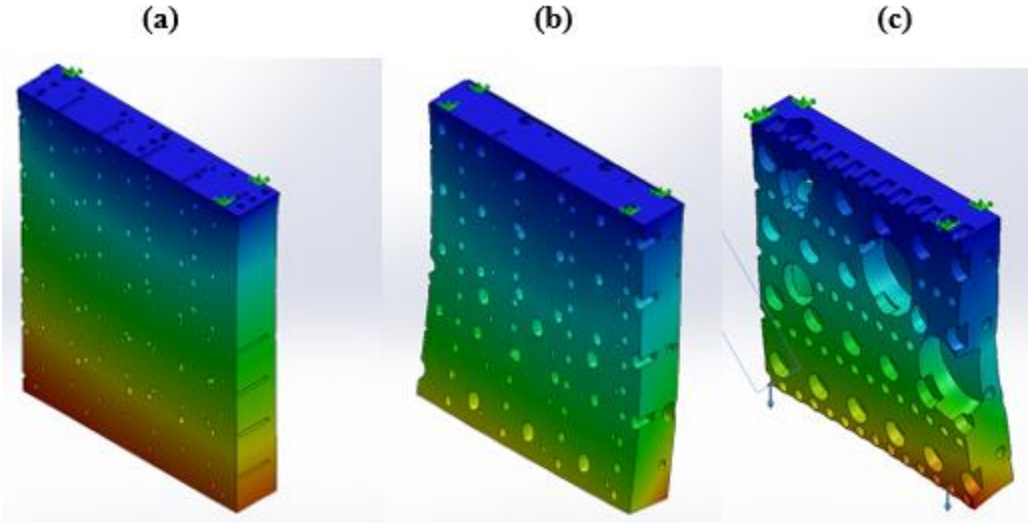

Figure 4.7: *Displacement simulation images of: (a) PLA scaffold (b) PLA-PEG scaffold (c) PLA-PEG-Nanoparticles scaffolds during tension test.*

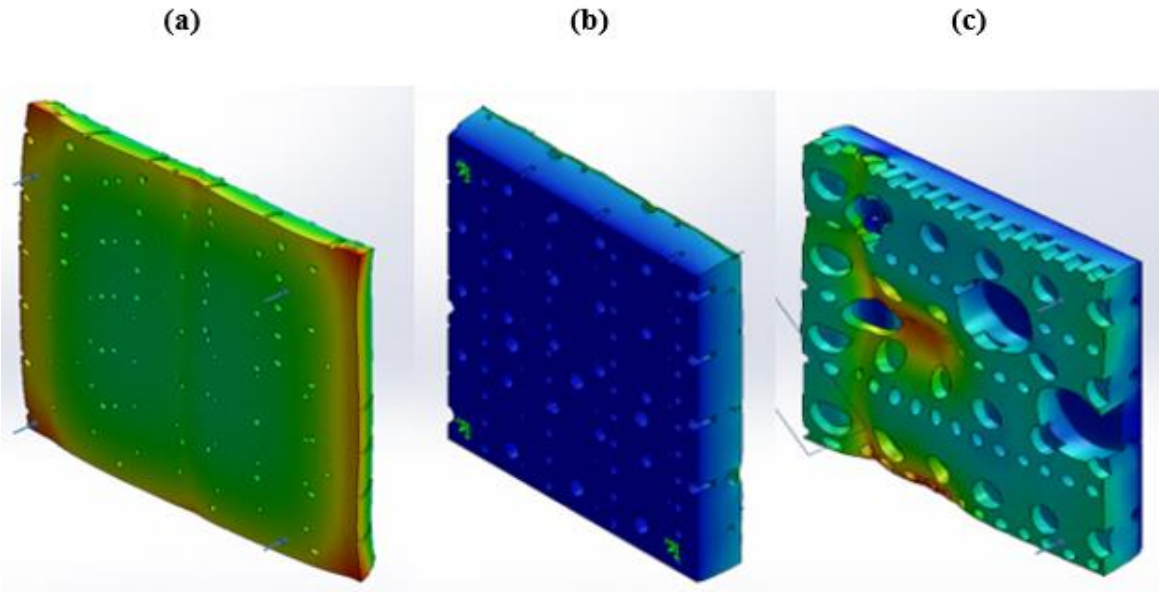

Figure 4.8: *Displacement simulation images of: (a) PLA scaffold (b) PLA-PEG scaffold (c) PLA-PEG-Nanoparticles scaffolds during compressive test.*

Table 4.3: *Table displaying maximum displacement, stress and strain during tension test.*

SAMPLE NAME	**Maximum Displacement (µm)**	**Stress Measured (MPa)**	**Strain Measured**
PLA	0.04043	0.8065	0.0004623
PLA-PEG	0.07141	1.928	0.001484
PLA-PEG-Nanoparticles	0.16610	1.537	0.001225

Table 4.4: *Table displaying maximum displacement, stress and strain during compression test.*

SAMPLE NAME	**Maximum Displacement (µm)**	**Stress Measured (MPa)**	**Strain Measured**
PLA	0.5407	53.81	0.03315
PLA-PEG	1.580	143.0	0.07951
PLA-PEG-Nanoparticles	2.241	110.8	0.08012

Chapter Five

5.0 Conclusions and Future Works

5.1 Remarks and Recommendation

The pursuit for cancer drugs for site targeting and specificity has yielded to several useful remarks. One, is the understanding that apart from the conventional methods of scaffold fabrication, which may be efficient but significantly expensive, one can embark in the fabrication through solvent casting process. The biopolymers used can ensure that tuneable characteristics such as biodegradation, biocompatibility, porosity, and hydrophilicity are controlled to fit a precise biological task.

The mutable nature of cancerous cells had led to a perpetual demand for new cancer drugs that would be locally and controllably administered. As part of this project, an experimental drug , Dichapetalin M, was analysed against an industrially available drug, Tamoxifen. This experimental drug exhibited desirable preliminary characteristics such as transient drug release and the Higuchi model of release which generally agree with the controllability requirement for locally delivered drugs.

Mechanical analysis of the samples informed us that the inclusion of PEG not only promotes hydrophilicity into the sample, but also plays part in the increase of pores sizes and pores density. PEG and Fe_3O_4 nano powder plays a crucial role in increasing the overall pore diameter at physiological conditions (37℃, pH 7.4, and 60 rpm). Drug release was enhanced by natural diffusion through the porous matrices of the scaffolds. Hydrolysis also plays a major role in drug diffusion, especially when the polymer gets soaked in phosphate buffer saline solution.

The significance of mechanical and structural changes in the scaffold enhances the goal of attaining properties of the device that are close enough to the properties of a normal human tissue.

5.2 Limitations

Throughout the project several limitations managed to squeeze their way into resisting the expected progress rate or the expected outcome.

The manual grinding of porogen and cutting of PLA into pellets proved to be exceedingly time consuming. Both activities took a duration of one week to accomplish them. Had there been a machine, in the proximity of my reachability, that would have grinded the table salt into fine particulates, that would have been appreciated.

The process of liquifying PLA pellets proved to be quite time consuming. I am hopeful, there could be more efficient method of liquefying PLA pellets soon.

Inclusion of the porogen (grinded table salt) into the polymeric liquid proved to be another limitation to an expected outcome. The sprinkling of porogen into and onto the pouring polymeric liquid was somewhat uncontrolled. The uneven sprinkling of the porogen led to uneven distribution of pores in the sample. Thus, the uneven distribution cause uneven pores creation which might affect the transportation of localized drugs, nutrients, and oxygen to adjacent body tissues.

Aside the practical limitations, the outbreak of Coronavirus disease-19 undeniably did affect the project progress pace as well as changing the direction onto which the project was initially intended. However, this experience has taken us into a place of knowing that it is possible to work even in the limited conditions if determination is still intact.

5.3 Future works

Dynamic effects of nanoparticles on laser heating and drug release is an area that should be investigated. This will provide insights on how nanoparticles-based porous scaffold structures could enhance localized temperature to induce apoptosis in cancerous cells. The drug loaded scaffolds containing nanoparticles can provide a synergy to both hyperthermia and localized drug delivery.

Investigation on the biochemical degradation of the scaffolds via mass loss is another area that can be worked on. This would be done through determining the degradation rates, mechanism of degradation, and structural integrity of the scaffold (mechanical properties).

A series of mechanical tests such as hardness, stiffness, tensile and compression strength, can also be manually done at regular interval during degradation and the results received would be translated into a software of choice for the goal of mechanically simulating the static conditions of the scaffold in terms of stress distribution, deformation and elastic strains.

Cell seeding and biocompatibility tests can also be carefully carried out on the scaffolds which could be followed by cell viability (determination of dead and living cells in a sample) studies via laser application and controlled drug release.

References

[1] W. Street. Cancer Facts and Figures (2019) 76.

[2] T. J. Mitchison and E. D. Salmon. Mitosis: a history of division, *Nat Cell Biol*. Vol. 3 (1) (2001) E17-E21.

[3] D. Green. Means to an End: Apoptos and Other Cell Death Mechanisms. Cold Spring Harbor Laboratory Press, (2010).

[4] A. I. McClatchey and A. S. Yap. Contact inhibition (of proliferation) redux, *Current Opinion in Cell Biology*. Vol. 24 (5) (2012) 685-694.

[5] A. Ilbawi, Cancer. *World Health Organization*. https://www.who.int/westernpacific/health-topics/cancer. Date access: 18-Oct-2019.

[6] C. Choy. The Metastatic Cascade: A Cell's Journey from One Organ to Another, *Metavivo*, (2015). https://www.metavivor.org/research/research-news/the-metastatic-cascade-a-cells-journey-from-one-organ-to-another/. Date access: 18-Oct-2019.

[7] "What is Cancer Cancer Research UK" Available: https://www.cancerresearchuk.org/about-cancer/what-is-cancer. Date access: 18-Oct-2019

[8] Types of Cancer Treatment. *National Cancer Institute*, Available: https://www.cancer.gov/about-cancer/treatment/types (2017).

[9] Y. Danyuo, J. D. Obayemi, S. Dozie-Nwachukwu, C. J. Ani, O. S. Odusanya, Y. Oni, N. Anuku, K. Malatesta, W. O. Soboyejo. Prodigiosin release from an implantable biomedical device: kinetics of localized cancer drug release, *Mater. Sci. and Eng. C*. Vol. 42 (2014) 734-745.

[10] Y. Danyuo, J. D. Obayemi, S. Dozie-Nwachukwu, C. J. Ani, O. S. Odusanya, Y. Oni, N. Anuku, K. Malatesta, W. O. Soboyejo. Prodigiosin Release from an Implantable

Biomedical Device: Effect on Cell Viability. Advanced Materials Research. Vol.11 (2016) 3-18.

[11] F. J. O'Brien. Biomaterials and scaffolds for tissue engineering, Materials Today. Vol. 14 (32) (2011) 88-95.

[12] S. J. Hollister. Porous scaffold design for tissue engineering, *Nature Materials*. Vol. 4 (2005) 518-524.

[13] L. Moroni, J. R. de Wijn, C. A. van Blitterswijk. 3D fibre-deposited scaffolds for tissue engineering: Influence of pores geometry and architecture on dynamic mechanical properties, *Biomaterials*. Vol. 27 (7) (2006) 974-985.

[14] T. Garg, O. Singh, S. Arora, and R. Murthy. Scaffold: a novel carrier for cell and drug delivery. *Crit Rev Ther Drug Carrier Syst*. Vol. 29 (1) (2012) 1-63.

[15] D. Sin, X. Miao, G. Liu, F. Wei, G. Chadwick, C. Yan, T. Friis. Polyurethane (PU) scaffolds prepared by solvent casting/particulate leaching (SCPL) combined with centrifugation, *Materials Science and Engineering: C*. Vol. 30 (1) (2010) 78-85.

[16] N. Nishida, H. Yano, T. Nishida, T. Kamura, and M. Kojiro. Angiogenesis in Cancer, *Vasc. Health Risk Manag*. Vol. 2 (3) (2006) 213-219.

[17] S. Pruthi, "Diagnosis and treatment - Mayo Clinic," 2011. [Online]. Available: https://www.mayoclinic.org/diseases-conditions/cancer/diagnosis-treatment/drc-20370594?p=1. [Accessed: 10-Nov-2019].

[18] "Chemotherapy: What it is, what to expect, side effects, and outlook." [Online]. Available: https://www.medicalnewstoday.com/articles/158401.php#what_to_expect. [Accessed: 03-Nov-2019].

[19]"Radiation Therapy Basics." [Online]. Available: https://www.cancer.org/treatment/treatments-and-side-effects/treatment-types/radiation/basics.html. [Accessed: 03-Nov-2019].

[20] M. Hurwitz and P. Stauffer, "Hyperthermia, Radiation and Chemotherapy: The Role of Heat in Multidisciplinary Cancer Care," *Seminars in Oncology*, vol. 41 (6(2014) 714-729.

[21] J. J. Skitzki, E. A. Repasky, and S. S. Evans, "Hyperthermia as an immunotherapy strategy for cancer," *Curr Opin Investig Drugs*, vol. 10 (6) (2009) 550-558.

[22] "Why and How Hair Loss Happens During Breast Cancer Treatment," *Breastcancer.org*, 12-Jun-2019. https://www.breastcancer.org/tips/hair_skin_nails/hair_loss. [Accessed: 09-Nov-2019].

[23] S. Pruthi, "Recurrent breast cancer - Symptoms and causes," *Mayo Clinic*. [Online]. Available:https://www.mayoclinic.org/diseases-conditions/recurrent-breast-cancer/symptoms-causes/syc-20377135. [Accessed: 10-Nov-2019].

[24] H. (Jack) West, "Chemotherapy-Induced Hair Loss (Alopecia)," *JAMA Oncol*, vol. 3(8) (2017) 1147-1147.

[25] K. N. Bitar and E. Zakhem, "Design Strategies of Biodegradable Scaffolds for Tissue Regeneration," Biomed Eng. Comput. Biol. vol. 6 (2014) 13-20.

[26] P. X. Ma, "Scaffolds for tissue fabrication," Materials Today, vol. 7 (5) (2004) 30-40.

[27] F. J. O'Brien, "Biomaterials & scaffolds for tissue engineering," *Materials Today*, vol. 14(3) (2011) 88-95. Doi: 10.1016/S1369-7021(11)70058-X.

[28] M. Tanaka, K. Sato, E. Kitakami, S. Kobayashi, T. Hoshiba, and K. Fukushima, "Design of biocompatible and biodegradable polymers based on intermediate water concept," *Polym J*, vol. 47(2) (2015) 114-121. Doi: 10.1038/pj.2014.129.

[29] M. Krebsz, T. Pasinszki, T. T. Tung, and D. Losic, "14 - Development of Vapor/Gas Sensors From Biopolymer Composites," in *Biopolymer Composites in Electronics*, K. K. Sadasivuni, D. Ponnamma, J. Kim, J.-J. Cabibihan, and M. A. AlMaadeed, Eds. Elsevier (2017) 385-403.

[30] P. K. Manvi, M. Beckers, B. Mohr, G. Seide, T. Gries, and C.-A. Bunge, "Chapter 3 - Polymer fiber-based biocomposites for medical sensing applications," in *Materials for Biomedical Engineering*, V. Grumezescu and A. M. Grumezescu, Eds. Elsevier (2019) 57-88.

[31] P. Dobson, H. Jarvie, and S. King, "Nanoparticle, Definition, Size Range, & Applications," *Encyclopedia Britannica* (2019).

[32] T. J. Webster, "Nanomedicine: what's in a definition?" *Int J Nanomedicine*, vol. 1(2) (2006) 115-116.

[33] N. Sahai, N. Ahmad, and M. Gogoi, "Nanoparticles Based Drug Delivery for Tissue Regeneration Using Biodegradable Scaffolds: a Review," *Curr Pathobiol Rep* vol. 6(4) (2018) 219-224. Doi: 10.1007/s40139-018-0184-8.

[34] F. Chen and W. Cai, "Nanomedicine for Targeted Photothermal Cancer Therapy: Where Are We Now?" *Nanomedicine (Lond)*, vol. 10(1) (2015) 1-3. Doi: 10.2217/nnm.14.186.

[35] C. Dowding, "19 - Laser ablation," in *Advances in Laser Materials Processing*, J. Lawrence, J. Pou, D. K. Y. Low, and E. Toyserkani, Eds. Woodhead Publishing (2010) 575-628.

[36] H. Jelínková, "1 - Introduction: the history of lasers in medicine," in *Lasers for Medical Applications*, H. Jelínková, Ed. Woodhead Publishing, (2013) 1-13.

[37] E. Schena, P. Saccomandi, and Y. Fong, "Laser Ablation for Cancer: Past, Present and Future," *J Funct Biomater*, vol. 8(2) (2017). Doi: 10.3390/jfb8020019.

[38] R. Alteri, K. Mamta, L. Yadao, and C. Ogoro, “Ablation for Liver Cancer,” American Cancer Society (2019).

[39] L. A. Torre, R. L. Siegel, E. M. Ward, and A. Jemal, “Global Cancer Incidence and Mortality Rates and Trends-An Update,” Cancer Epidemiol Biomarkers Prev, vol. 25, no. 1, (2016) 16-27. Doi: 10.1158/1055-9965.EPI-15-0578.

[40] H. K. Shaikh, R.V. Kshirsagar, S.G. Patil. Mathematical models for drug release characterization: A review. World Journal of pharmacy and pharmaceutical sciences. 4(04) (2015) 324-338.

[41] Y. Danyuo, O. Oberaifo, J. D. Obayemi, S. Dozie-Nwachukwu, C. J. Ani, O. S. Odusanya, M. G. Zebaze Kana, K. Malatesta and W. O. Soboyejo. Extended pulsated drug release from PLGA-based minirods. J. of Mater. Sci.: Mater. in Med. (JMSM). 28 (2017) 61.

[42]“What is a Good R-squared Value?,” Statology, Feb. 24, 2019. https://www.statology.org/good-r-squared-value/ (accessed May 28, 2020).

[43] M. L. Bruschi, Ed., “5 - Mathematical models of drug release,” in Strategies to Modify the Drug Release from Pharmaceutical Systems, Woodhead Publishing (2015) 63-86.

[44] S. Dash, P. N. Murthy, L. Nath, and P. Chowdhury, “Kinetic modeling on drug release from controlled drug delivery systems.,” Acta poloniae pharmaceutica (2010).

[45] J. Siepmann and N. A. Peppas, “Higuchi equation: Derivation, applications, use and misuse,” International Journal of Pharmaceutics, vol. 418(1) (2011) 6-12. Doi: 10.1016/j.ijpharm.2011.03.051.

Appendix A

Materials and Equipment Used

Materials and Equipment	Description
	LARK Ethanol AR (2.5L), 99.9%, MW=46g/mol Product code; LA-1891-2.5L LARK CIENTIFICO Delhi-110034, India
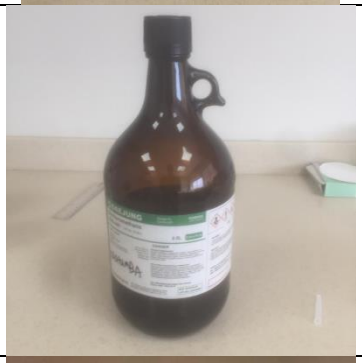	DAEJUNG Dichloromethane (2.5L) DAEJUNG CHEMICALS &METALS CO. LTD Gyeonngi-do, Korea
	Distilled water (25L) FINAP ENTERPRISE 13 Hearts Lane Kokomlemle, Accra, GT Accra, Ghana

		Kermel Sodium Chloride (500g, MW= 101.96g/mol) BDH Laboratory Supplies Poole Bh 15 1 TD, England
		Micro PIPETTE Pipette (0-50µL)
	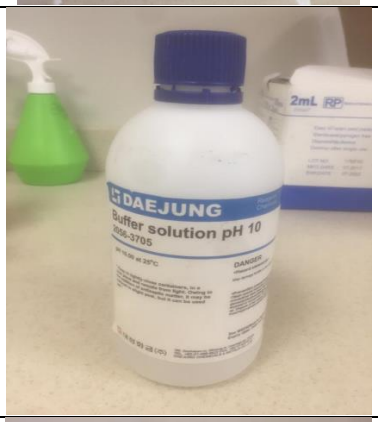	DAEJUNG Buffer solution Ph 10 at 25^0C (500mL) DAEJUNG CHEMICALS &METALS CO. LTD Gyeonngi-do, Korea
	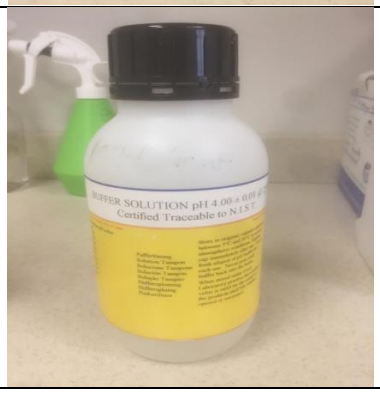	Reagecon Buffer Solution pH 4.00 ± 0.01 at 25^0C (500mL) Reagecon Ireland

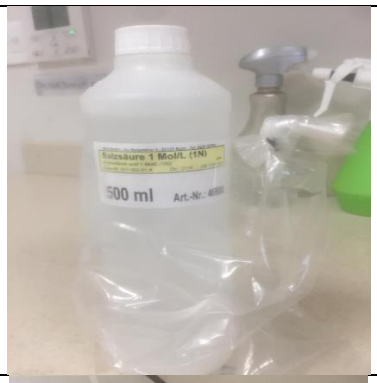	Salzsäure Hydrochloric Acid (1 mol/L) SCS Schulchemieservice GmbH At Burgweiher 3 53123 Bonn, Germany
	KERBO Hotplate Stirrer Model: MX-HS-16
	ESCO Laboratory Fume Hood FrontierDUO
	Benchmark Incu-shaker Mini

	JENWAY Life science spectrophotometer Genova Bio
	Mettler Toledo® (ME 103) Analytical balance Mettler-Toledo International, Inc Columbus, Ohio, USA
	AG ADVANGENE 12well, surface-treated tissue culture plate Life Science Plasticware 21N. Skokie Hwy, Suite 104,Lake Bluff, Illinois 60044, USA
	Xinxing Qualitative Filter Paper (diameter=110mm)
	Greiner Test tube (15 mL)

		Euro-Ject-III Single use syringe (5mL) Changzhou Huichun Medical Equipment Co. LTD Changzhou, Jiangsu, China
		ULAB Microcentrifuge Tube (1.5mL) ULAB China
	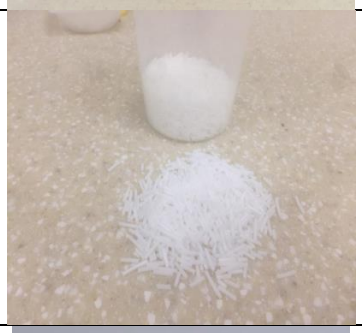	Poly-lactide-acid (PLA) pellets
	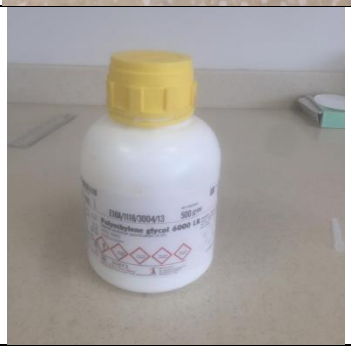	SDFCL Poly-Ethylene-Glycol (PEG) 500g S D FINE-CHEM LTD 1502, Marathon Icon, Lower Parel, Mumbai-400 013, India

		Polyvinylpyrrolidone (PVP) ACROS ORGANICS New Jersey, USA
		ALDRICH Iron (II,III) oxide, nanopowder SIGMA-ALDRICH Inc St. Louis, MO 63103, USA
		Table salt(NaCl)
	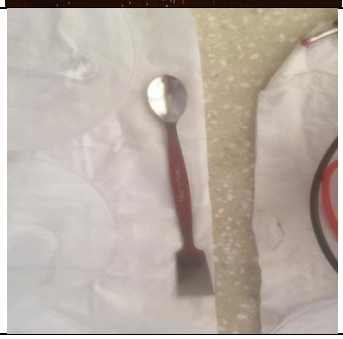	Spatula

		Beaker (400mL, 500mL, 600mL)
		Surgical Blades
		Lab Coat
		Hand Gloves
		Nose masks

		Glass petri dish (30mm diameter)
	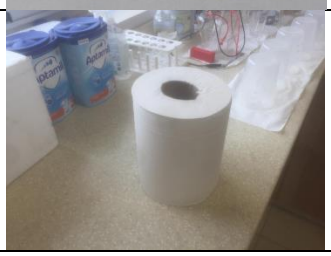	Paper towel

Appendix B

Absorbance against Duration data

SAMPLE A

DAY	A1	A2	A3	A
0	1.081	1.081	1.081	1.081
1	0.132	0.239	0.276	0.216
2	0.133	0.131	0.171	0.145
3	0.165	0.072	0.057	0.098
4	0.063	0.082	0.067	0.071
5	0.048	0.050	0.007	0.035
6	0.035	0.074	0.074	0.061
7	0.256	0.070	0.090	0.139
8	0.108	0.066	0.079	0.084
9	0.097	0.198	0.064	0.120
10	0.033	0.026	0.046	0.035
11	0.059	0.069	0.065	0.064

SAMPLE B

DAY	B1	B2	B3	B
0	0.581	0.581	0.581	0.581
1	0.329	0.266	0.296	0.297
2	0.111	0.095	0.161	0.122
3	0.000	0.031	0.268	0.100
4	0.094	0.066	0.102	0.087
5	0.041	0.056	0.018	0.038
6	0.188	0.057	0.077	0.107
7	0.167	0.135	0.121	0.141
8	0.117	0.089	0.077	0.094
9	0.152	0.205	0.089	0.149
10	0.080	0.033	0.080	0.064
11	0.110	0.131	0.121	0.121

SAMPLE C

DAY	C1	C2	C3	C
0	1.081	1.081	1.081	1.081
1	0.267	0.304	0.264	0.278
2	0.230	0.176	0.193	0.200
3	0.026	0.023	0.069	0.039
4	0.108	0.126	0.161	0.132
5	0.108	0.035	0.099	0.081
6	0.077	0.083	0.086	0.082
7	0.120	0.197	0.115	0.144
8	0.098	0.051	0.087	0.079
9	0.124	0.101	0.145	0.123
10	0.038	0.025	0.063	0.042
11	0.113	0.127	0.107	0.116

SAMPLE E

DAY	E1	E2	E3	E
0	0.581	0.581	0.581	0.581

1	0.031	0.312	0.290	0.211
2	0.172	0.179	0.212	0.188
3	0.094	0.013	0.051	0.053
4	0.139	0.140	0.176	0.152
5	0.034	0.070	0.037	0.047
6	0.134	0.123	0.168	0.142
7	0.153	0.139	0.106	0.133
8	0.086	0.158	0.115	0.120
9	0.105	0.120	0.100	0.108
10	0.091	0.092	0.103	0.095
11	0.109	0.162	0.013	0.095